



PERGAMON

Available online at [www.sciencedirect.com](http://www.sciencedirect.com)

SCIENCE @ DIRECT®

Polyhedron 22 (2003) 1883–1888



POLYHEDRON

[www.elsevier.com/locate/poly](http://www.elsevier.com/locate/poly)

# Possible flat-band ferromagnetism in an organic polymer

Ryotaro Arita<sup>a,\*</sup>, Y. Suwa<sup>b</sup>, K. Kuroki<sup>c</sup>, H. Aoki<sup>a</sup>

<sup>a</sup> Department of Physics, University of Tokyo, Hongo, Tokyo 113-0033, Japan

<sup>b</sup> Advanced Research Laboratory, Hitachi Ltd., Kokubunji, Tokyo 185-8601, Japan

<sup>c</sup> Department of Applied Physics and Chemistry, University of Electro-Communications, Chofu, Tokyo 182-8585, Japan

Received 6 October 2002; accepted 10 February 2003

## Abstract

Motivated from the flat-band form magnetism conceived in the physics of correlated electrons; we predict that a polymer of five-membered rings can exhibit band (i.e. itinerant) ferromagnetism. We have first identified that the right material having a flat one-electron dispersion should be polyaminotriazole, for which we have performed a generalized gradient approximation (GGA) calculation based on the spin density functional. The result shows that the ground state is indeed ferromagnetic when the flat band is made half-filled. From the structural optimization, we also show that the magnetism overcomes the Peierls instability, unlike conjugated polymers such as polyacetylene. We have also confirmed that the mechanism for the ferromagnetism is the flat-band ferromagnetism by comparing the first-principles wavefunction with those in the Hubbard model. Possibility of the bulk ferromagnetism for the three dimensional polyaminotriazole crystal with chemical carrier doping is also discussed.

© 2003 Elsevier Science Ltd. All rights reserved.

**Keywords:** Itinerant ferromagnetism; Organic polymer; Flat band; Polyaminotriazole; Molecular crystal; First-principles calculation

## 1. Introduction

Ferromagnetism in *purely* organic materials is an issue of great interest and an enormous amount of experimental and theoretical studies have been carried out. A recent example is TDAE-C<sub>60</sub>; where unpaired electrons localized on C<sub>60</sub> molecules become ferromagnetic below  $T = 16$  K, and the magnetic behavior can be described in terms of the Heisenberg model [1]. Ferromagnetism in *itinerant* electron systems, on the other hand, is entirely a different issue, and organic metals that exhibit *band ferromagnetism* have not been synthesized. Whether we can have itinerant ferromagnetism in purely organic materials has yet to be clarified [2], and thus remains a fundamental question from both physical and quantum chemical points of view.

Theoretically, the Hubbard model is the simplest possible one in discussing itinerant ferromagnetism in

$\pi$ -electron systems in polymers, since tight-binding picture for these systems is quite valid in general.

As for theoretical studies on the ferromagnetism in the Hubbard model, various approaches have been taken by various authors since the 1960s [4–6]. A new turn of events took place in the 1980s when Lieb, and later Mielke and independently Tasaki, proved rigorously that, when the one-electron band structure contains a special kind of flat (i.e. dispersionless) band, the repulsive electron–electron interaction should guarantee fully spin-polarized ground states when the flat band is half-filled [3]. An important point is that the flat band is totally different from the narrow-band limit—the band can be flat even when the transfer energy,  $t$ , is finite. A second important point is that the flat band does not automatically imply ferromagnetism. Mielke and Tasaki have shown that what they call the local connectivity condition for the basis functions in the flat band is required. When this is satisfied, adjacent “Wannier” orbitals have to overlap no matter how they are combined to minimize the orbit size, which is why spins have to align due to Pauli’s principle [7].

In the present study, motivated from this flat-band ferromagnetism, we propose a new possibility of the

\* Corresponding author. Tel.: +81-3-5841-4220; fax: +81-3-5841-4063.

E-mail address: [arita@cms.phys.s.u-tokyo.ac.jp](mailto:arita@cms.phys.s.u-tokyo.ac.jp) (R. Arita).

band ferromagnetism in a purely organic polymer. First question would be: why organic polymers? Mielke–Tasaki’s orbits are constructed from interferences between nearest-neighbor and second neighbor transfers, and this requires special lattice structures, which is rather difficult to realize in spatial dimensions greater than one. In quasi one-dimensional systems we can conceive lattices having flat bands relatively easily, so that we propose that organic polymers are promising candidates to realize the flat-band ferromagnetism.

Among various polymers, polymers comprising five-membered rings merit special attention, because the tight-binding model on the chain of odd-membered rings tend to realize flat band conditions (although of course the chain of odd-rings is not a sufficient condition). For the five-membered rings we can illustrate this in Fig. 1, where the flat bands appearing in appropriate, realistic conditions have wavefunctions satisfying the local connectivity condition (overlapping “Wannier” orbitals). Another reason, for magnetism, why odd-membered rings are desirable is that antiferromagnetism, with which ferromagnetism has to compete, tends to be suppressed due to frustration.

By the first-principle band calculation, we find that a chain of five membered rings with a right choice of the functional group (polyaminotriazole) has indeed an almost completely flat band. We then show that the ground state is ferromagnetic when the band is hole doped to be half-filled. It is also shown that the magnetism overcomes the Peierls instability [8]. We confirm that the magnetism really has to do with the Mielke–Tasaki mechanism by mapping the  $\pi$ -orbital system to the Hubbard model.

## 2. Method

The band structure is obtained with a first principles calculation within the framework of the generalized gradient approximation based on the (spin) density functional theory (which we call GGA-(S)DFT) [9]. We adopt the exchange-correlation functional introduced by Perdew et al. [9] and ultra-soft pseudo-potentials [10,11] in a separable form.

The wavefunctions are expanded by plane waves up to a cut-off energy of 20.25 Ry. Chemically, five-membered rings usually alternate their directions in a chain (see the



Fig. 1. The chain of five-membered rings, where the enclosed areas indicate “Wannier” orbitals that satisfy the local connectivity condition.

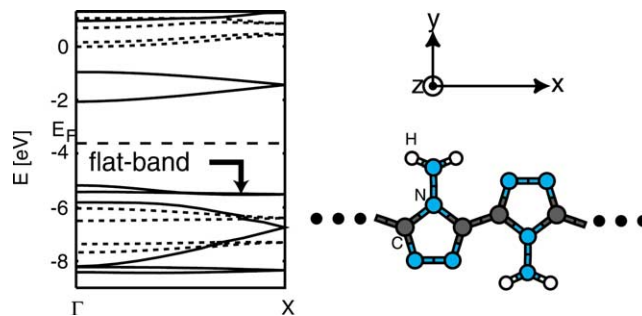


Fig. 2. The band structure (left panel) and the optimized atomic configuration (right) for the (undoped) polyaminotriazole obtained by the GGA-DFT. The solid (dotted) lines represent bands having  $\pi$  ( $\sigma$ ) character.

right panel of Fig. 2), so that there are two rings in a unit cell with the Brillouin zone folded. In directions perpendicular to the chain we take a repeated-chain model with a sufficiently large repeat distance. The atomic configuration as well as the unit cell size along the chain is optimized to minimize the ground state energy with the conjugate gradient scheme [12].

## 3. GGA results

We start with a search for the case of flat bands by scanning various five-membered polymers, i.e. polypyrrole, polythiophene, polytriazole. We have found that  $\pi$ -electron systems in these polymers do not have any flat bands. It should be noted that a five membered ring is by no means a sufficient condition for a flat band, so that it is not too surprising that the flat band is rather hard to realize in real organic polymers.

Next, we attach some functional groups, which are K, Na,  $\text{NH}_2$ , OH, Cl, F,  $\text{HSO}_3$ ,  $\text{NO}_2$ , CN, and COOH [13] to each ring in order to tune site energies and/or transfer integrals. We have found among the polymers investigated here that polyaminotriazole (poly(4-amino 1,2,4-triazole)) to be precise, see inset of Fig. 2) hits the right condition. In Fig. 2, we can see that the top valence band (with two branches due to the above-mentioned band folding) has little dispersion ( $\sim 0.1$  eV).

While the highest valence band of polyaminotriazole is fully filled, positive carrier must be doped to this band to induce the flat band ferromagnetism. Experimental feasibility for the carrier doping will be discussed later. We have carried out a GGA-SDFT calculation [9] for the doped polyaminotriazole starting with three (i.e. paramagnetic, ferromagnetic and antiferromagnetic) initial states, and compare the total energy of these states. We have focused on the situation where the highest valence band is hole-doped to be half-filled (i.e. the upper branch arising from the band folding empty). When we introduce the holes to the system, a uniform negative background charge is introduced so as to

satisfy the charge neutrality condition. Note that polyaminotriazole is not a conjugated polymer, in contrast to polyacetylene, where the double bonds resonating with single bonds cause strong Peierls instability, so that the application of DFT is not a subtle problem in that context (Fig. 3). Even when the flat band is doped, holes are doped into the Mielke–Tasaki orbitals satisfying the connectivity condition, so that the localized double bonds are again absent.

In Fig. 4, we show the result when we take the polarized state as the initial state. The optimized state remains polarized, where the splitting between the majority-spin and minority-spin bands is  $\simeq 1$  eV. It should be noted that this value is similar to the exchange splitting estimated in [14] for the flat-band ferromagnetism first proposed for an atomic quantum wire [7].

Generally, one-dimensional metals are unstable against the *Peierls instability*, where the electronic energy is lowered at the cost of the lattice distortion. Thus we have to check whether the energy gained due to the spin polarization overcomes the Peierls instability. In the left panel of Fig. 5, we show the result obtained by the GGA-DFT where the global minimum of the total energy is higher than that of the polarized optimized state in the GGA-SDFT calculation by  $\simeq 400$  meV. Note that although Peierls distortion is allowed in the GGA-DFT, we can see that the Peierls splitting at X is negligibly small. Physically, this should be because  $\sigma$ -bonds which form the backbone of the structure are so rigid that they can cope with the Peierls instability.

If we allow the spatial distributions of up and down spins to be different in the GGA-SDFT starting from an initially unpolarized state, the resulting band structure has a wide gap at the Fermi level (right panel of Fig. 5), which we attribute to an antiferromagnetic gap. Although the total energy of the antiferromagnetic state is lower than that for the uniformly zero spin density (the left panel of Fig. 5), the energy is higher than that of the optimized polarized state (Fig. 4) by  $\simeq 50$  meV. Thus we can conclude that the true ground state in the GGA-SDFT is the polarized one.

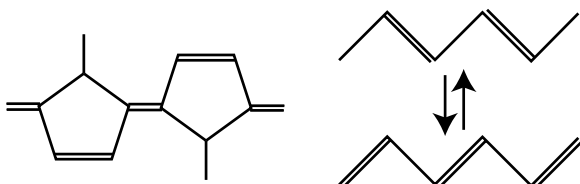


Fig. 3. The double bonds in polyaminotriazole (left) and polyacetylene (right).

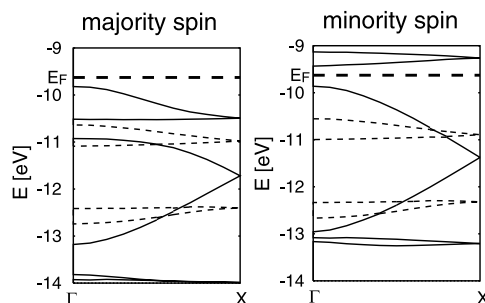


Fig. 4. The band structure of the *doped* system with an optimized structure obtained with the GGA-SDFT. The solid (dotted) lines represent the bands having  $\pi$  ( $\sigma$ ) character.

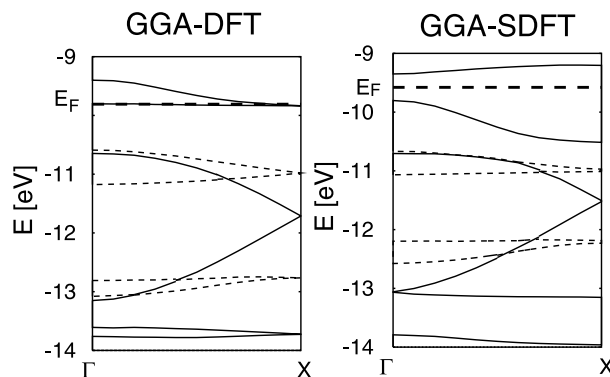


Fig. 5. Band structure for the *doped* system optimized by allowing the Peierls distortion in the GGA-DFT (left panel), and that for the antiferromagnetic state obtained with the GGA-SDFT (right).

#### 4. Mapping to the Hubbard model and the magnetic phase diagram

Let us confirm whether the flat band mechanism a la Mielke–Tasaki for the Hubbard model has to do with the polarization obtained in the GGA-SDFT calculation. For this purpose, we first map the  $\pi$  electron systems to the tight-binding model, whose Hamiltonian is  $\mathcal{H}_0 = -\sum_{ij\sigma} t_{ij} c_{i\sigma}^\dagger c_{j\sigma} + \sum_i \epsilon_i n_i$  in the standard notation (see the right panel of Fig. 6).

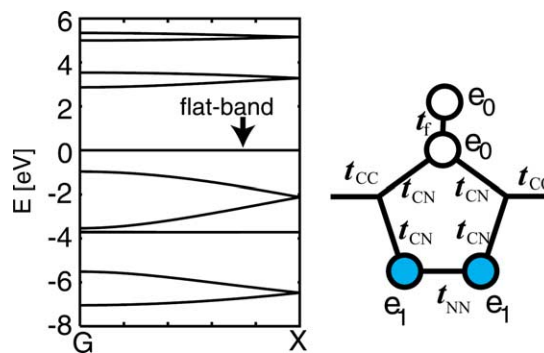


Fig. 6. The band dispersion of the tight-binding model with  $\epsilon_0 = -1.43$  eV,  $\epsilon_1 = -0.5$  eV,  $t_{CN} = t_{CC} = t_f = 2.5$  eV, and  $t_{NN} = 3.0$  eV. To facilitate comparison with Fig. 2, we have folded the band to have a two-ring unit cell.

The parameters are determined as follows. As for the transfer integrals, we calculate those from the energy difference between the bonding and anti-bonding  $\pi$ -orbitals at Brillouin zone center and edges. The nitrogen site energies ( $c$ 's) as measured from that for C are taken from the energy levels of isolated atoms. The obtained figures are:  $t_{CN} \simeq t_{CC} \simeq t_t = 2.5$  eV,  $t_{NN} = 3\text{--}4$  eV,  $\epsilon_0 \simeq \epsilon_1 = -1 \sim -2$  eV. We depict the band structure for this tight-binding model in the left panel of Fig. 7. We can see that it reproduces the features of the band for  $\pi$ -electrons in polyaminotriazole (Fig. 7). To check the connectivity condition we have to look at the wavefunctions on the flat band. Fig. 7 shows that the wavefunctions in the tight-binding model capture the features of those in the GGA-DFT result for polyaminotriazole.

Let us move on to the magnetic phase diagram—namely the question of how strong the interaction has to be to have ferromagnetism. In the presence of the Hubbard repulsion,  $\mathcal{H}_U = U \sum_i n_{i\uparrow} n_{i\downarrow}$ , we show the phase diagram against  $U$  and  $\epsilon_1$  in Fig. 8, which is obtained with an exact diagonalization calculation for a 12 site (2 unit-cell) Hubbard model for  $t_0 = 2.5$  eV with various values of  $t_{NN} = 3.0\text{--}4.0$  eV. As indicated by the inset,  $\epsilon_0$  is chosen throughout to satisfy the condition for the flat band,

$$\epsilon - \epsilon_1 = (1 - \epsilon)(t_{NN}^2 - (\epsilon - \epsilon_1)^2) - t_{NN},$$

$$(\epsilon - \epsilon_1 + t_{NN})/(1 - \epsilon) = -t_{NN}/(\epsilon_0 - \epsilon) - t_{NN}(\epsilon - \epsilon_0),$$

where  $\epsilon$  is the eigenenergy of the flat band and  $t_{CN} =$

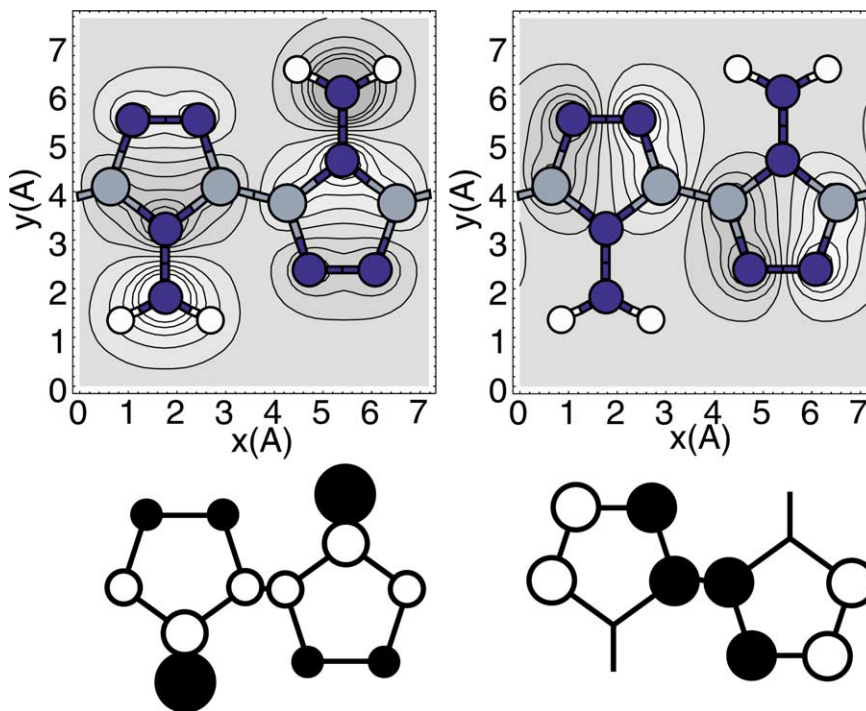


Fig. 7. Bloch wavefunctions (top panels) on the flat  $\pi$ -electron bands at  $\Gamma$  in polyaminotriazole (Fig. 2) obtained with the GGA-DFT as compared with the corresponding ones (bottom) in the tight-binding model (Fig. 6). Left/right panels correspond to the two eigenstates at  $\Gamma$  (which are degenerated in the folded flat band). White/black regions (or circles) represent the sign of the wavefunction, while the size of the circles the amplitude.

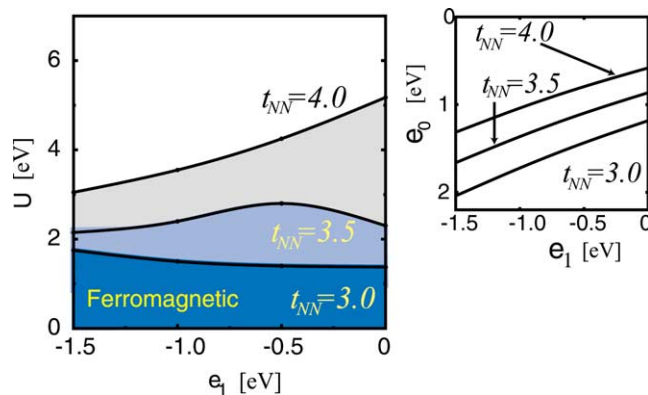


Fig. 8. Phase diagram for the Hubbard model on a lattice depicted in Fig. 6 against  $U$  and  $\epsilon_1$  for various values of  $t_{NN}$  for  $t_0 = 2.5$  eV. The inset shows the relation between  $\epsilon_1$  and  $\epsilon_0$  to realize the flat band.

$t_{CC} = t_0 (= 1$  here) is assumed for simplicity. We can see that we have a ferromagnetic phase *unless* the repulsion is too strong (i.e.  $U < U_c$  with  $U_c = 2\text{--}5$  eV). Namely, not only a weak  $U$  suffices, but also a larger  $U$  actually destroys ferromagnetism. Physically, ferromagnetism in the Mielko–Tasaki mechanism is guaranteed for  $0 < U \leq \infty$  when the flat band is the bottom band. When the flat band is sandwiched between dispersive ones, the theory becomes inapplicable. However, a numerical study for the case of a middle flat band in the context of a model atomic quantum wire [7] has shown that the ferromagnetism remains when  $U$  is below a critical value. The present result is consistent with this.



## 5. Ferromagnetism in the polymer crystal—an experimental feasibility

Let us finally comment on the robustness and experimental feasibility of the flat-band ferromagnetism. First, the one-electron dispersion does not have to be exactly flat to realize ferromagnetism, as confirmed from a number of studies [15,16]. Also, electron–electron interactions extending beyond the on-site do not necessarily degrade the ferromagnetism. This has been shown for the extended Hubbard model where the off-site repulsion  $V$  does not degrade, or in some situation even induces, the ferromagnetism [17]. We may expect that the ferromagnetism survives when the flat band is shifted away from the half-filling, as a numerical calculation [18] has indicated.

For experimental realization of the magnetism, bulk magnetization of three-dimensional crystal of the polymers is desirable. So we have considered crystals of polyaminotriazole chains, where herringbone arrays of polymers (Fig. 9(a)) with two chains per unit cell are assumed. It has been known that existing polymers such as polythiophen and polyphenylvinylene take such crystal structures, for which optical properties have been studied intensively [19,20]. We have performed a GGA-DFT calculation, and the preliminary result suggests that the band structure of polyaminotriazole crystal is similar to that of polyaminotriazole chain, which should be because the inter-chain coupling is weak.

We have then performed a GGA-SDFT calculation when the band filling in the three-dimensional crystal is changed by introducing a uniform negative background charge. Our preliminary result shows that there is a self-consistent ferromagnetic solution for the Kohn–Sham equation.

We envisage that the carrier doping to the crystal may be realized chemically by introducing some anions such as halogen atoms in the crystal. So we have finally performed a GGA-DFT calculation for Cl-doped polyaminotriazole crystal assuming the atomic positions of Cl as in Fig. 9(b). Our preliminary result indicates that

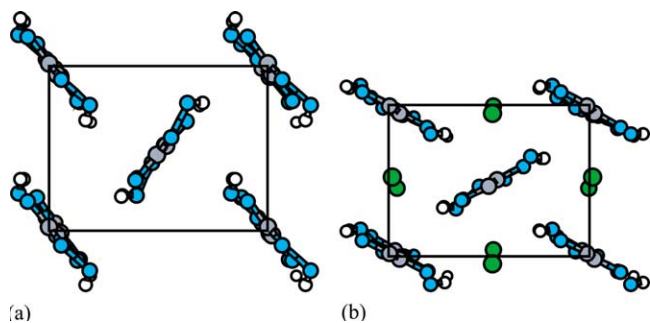


Fig. 9. The proposed crystal structure (top view) of polyaminotriazole crystal (a) and Cl-doped crystal (b) assumed for the band calculation. The unit cell is also indicated.

the flat band becomes half-filled as expected for four Cl atoms per unit cell (four five-membered rings).

## 6. Summary

We have found that the band width of the highest valence band of amino-polydiazole is nearly flat (with width  $\simeq 0(0.1 \text{ eV})$ ) within the framework of GGA-DFT. We have assessed the possibility of polarized ground state when the narrow band is doped to be half-filled by the GGA-SDFT calculations and the exact diagonalizations of the Hubbard model. The result suggests that, if the flat band of the amino-polydiazole is hole-doped, it will indeed be ferromagnetic at sufficiently low temperature. The mechanism of the polarization can understand in terms of Mielke and Tasaki's flat-band ferromagnetism in the Hubbard model.

## Acknowledgements

We would like to thank A. Koma, K. Saiki, T. Shimada, K. Ueno, Y. Shimoi, T. Hashizume and M. Ichimura for fruitful discussions. This work was supported in part by a Grant-in-Aid for Scientific Research and Special Coordination Funds from Ministry of Education of Japan, The GGA calculation was performed with TAPP (Tokyo Ab-initio Program Package), where R.A. and Y.S. would like to thank J. Yamauchi for technical advices. Numerical calculations were performed on SR8000 in ISSP, University of Tokyo.

## Appendix A

Here we present the atomic coordinates of the structure-optimized polyamino-triazole for a single chain (Fig. 2), crystallized form and Cl-doped crystal (Fig. 9), respectively. The linear dimension of the unit cell for the single chain is 7.197 Å along the chain ( $x$ ), 15.875 Å, 10.584 Å perpendicular to the chain (which are taken to be sufficiently large to suppress inter-chain interactions) and those for the crystal are 8.467, 6.350, 7.197 (Å) along  $x$ ,  $y$ , and  $z$ .

### (1) Single chain of polyaminotriazole

Atom species	$x$ (Å)	$y$ (Å)	$z$ (Å)	Atom species	$x$ (Å)	$y$ (Å)	$z$ (Å)
C	6.074	15.631	0.016	C	1.101	15.630	0.016
C	2.486	0.244	10.567	C	4.689	0.244	10.567
H	6.319	2.390	10.456	H	0.857	2.390	10.456
H	2.731	13.486	0.127	H	4.444	13.486	0.127
N	7.176	0.600	0.021	N	7.176	2.025	0.327

N	6.452	14.340	0.012	N	0.723	14.340	0.012	N	3.634	3.318	3.587	N	2.606	4.281	3.588
N	3.588	15.275	10.563	N	3.588	13.850	10.256	N	5.575	2.451	2.871	N	5.575	2.451	4.305
N	2.864	1.536	10.572	N	4.311	1.536	10.572	Cl	4.247	0.252	7.176	Cl	4.220	6.098	3.588
(2) Crystallized polyaminotriazole								Cl	8.466	2.918	7.176	Cl	8.467	3.432	3.588

Atom species	x (Å)	y (Å)	z (Å)	Atom species	x (Å)	y (Å)	z (Å)
C	8.304	6.185	6.072	C	8.304	6.185	1.104
C	0.163	0.165	2.484	C	0.163	0.165	4.692
C	4.106	3.366	6.072	C	4.106	3.366	1.104
C	4.361	2.984	2.484	C	4.361	2.984	4.691
H	1.576	1.822	6.321	H	1.576	1.822	0.855
H	6.891	4.528	2.733	H	6.891	4.528	4.443
H	5.557	1.158	6.325	H	5.557	1.158	0.850
H	2.910	5.192	2.737	H	2.910	5.192	4.438
N	0.367	0.488	7.176	N	0.995	1.801	7.176
N	7.479	5.187	6.465	N	7.479	5.187	0.711
N	8.100	5.862	3.588	N	7.472	4.550	3.588
N	0.988	1.163	2.877	N	0.988	1.163	4.299
N	4.622	2.700	7.176	N	5.705	1.728	7.176
N	3.312	4.388	6.466	N	3.312	4.388	0.710
N	3.845	3.650	3.588	N	2.762	4.622	3.588
N	5.155	1.962	2.878	N	5.155	1.962	4.298

## (3) Cl-doped crystallized polyaminotriazole

Atom species	x (Å)	y (Å)	z (Å)	Atom species	x (Å)	y (Å)	z (Å)
C	8.271	6.204	6.066	C	8.271	6.204	1.109
C	0.196	0.146	2.478	C	0.196	0.146	4.697
C	4.038	3.321	6.066	C	4.038	3.321	1.109
C	4.429	3.029	2.478	C	4.429	3.029	4.697
H	2.187	1.027	6.298	II	2.188	1.027	0.877
H	6.276	5.322	2.710	H	6.279	5.322	4.465
H	6.416	2.134	6.299	H	6.416	2.133	0.877
H	2.051	4.216	2.712	I!	2.050	4.216	4.464
N	0.598	0.141	7.175	N	1.634	1.095	7.176
N	7.123	5.630	6.459	N	7.123	5.630	0.717
N	7.868	6.209	3.587	N	6.833	5.256	3.588
N	1.343	0.720	2.871	N	1.343	0.720	4.305
N	4.832	3.033	7.175	N	5.861	2.069	7.176
N	2.892	3.899	6.459	N	2.892	3.899	0.717

## References

- [1] P.M. Allemand, K.C. Khemani, A. Koch, F. Wudl, K. Holczer, S. Donovan, G. Gruner, J.D. Thompson, *Science* 253 (1991) 301As for recent discovery of ferromagnets that exploit radicals, see A. Rajca, J. Wongsriratanakul, S. Rajca, *Science* 294 (2001) 1503..
- [2] Shima and one of the present authors have predicted that some graphites with superhoneycomb structure whose valence band is completely dispersionless will have net polarization [N. Shima, H. Aoki, *Phys. Rev. Lett.* 71 (1993) 4389], but this has to do with ferromagnetism, a kind of antiferromagnetism.
- [3] For reviews, see H. Tasaki, *Prog. Theor. Phys.* 99 (1998) 489; A. Mielke, H. Tasaki, *Commun. Math. Phys.* 158 (1993) 341.
- [4] M.C. Gutzwiller, *Phys. Rev. Lett.* 10 (1963) 159.
- [5] J. Kanamori, *Prog. Theor. Phys.* 30 (1963) 275.
- [6] J. Hubbard, *Proc. R. Soc. London, Ser. A* 276 (1963) 238.
- [7] R. Arita, K. Kuroki, H. Aoki, A. Yajima, M. Tsukada, S. Watanabe, M. Ichimura, T. Onogi, T. Hashizume, *Phys. Rev. B* 57 (1998) R6854.
- [8] R. Arita, Y. Suwa, K. Kuroki, H. Aoki, *Phys. Rev. Lett.* 88 (2002) 127202.
- [9] J.P. Perdew, K. Burke, Y. Wang, *Phys. Rev. B* 54 (1996) 16533.
- [10] D. Vanderbilt, *Phys. Rev. B* 41 (1990) 7892.
- [11] K. Laasonen, A. Pasquarello, R. Car, C. Lee, D. Vanderbilt, *Phys. Rev. B* 47 (1993) 10142.
- [12] J. Yamauchi, M. Tsukada, S. Watanabe, O. Sugino, *Phys. Rev. B* 54 (1996) 5586.
- [13] Y. Suwa, R. Arita, K. Kuroki, H. Aoki, unpublished.
- [14] S. Okada, A. Oshiyama, *Phys. Rev. B* 62 (2000) R13286.
- [15] K. Kusakabe, H. Aoki, *Phys. Rev. Lett.* 72 (1994) 144.
- [16] K. Pene, H. Shiba, F. Mila, T. Tsukagoshi, *Phys. Rev. B* 54 (1996) 4056.
- [17] R. Arita, Y. Shimoi, K. Kuroki, H. Aoki, *Phys. Rev. B* 57 (1998) 10609.
- [18] H. Sakamoto, K. Kubo, *J. Phys. Soc. Jpn.* 65 (1996) 3732.
- [19] G. Bussi, A. Ruini, E. Molinari, M.J. Caldas, P. Puschnig, C.A. Draxl, *Appl. Phys. Lett.* 80 (2002) 4118.
- [20] A. Ruini, M.J. Caldas, G. Bussi, E. Molinari, *Phys. Rev. Lett.* 88 (2002) 206403.